

## **Partial sulfur vacancy created by carbon-nitrogen deposition of MoS<sub>2</sub> for high-performance overall electrocatalytic water splitting**

*Wenxia Chen<sup>a\*</sup>, Wei Wei<sup>a</sup>, Kefeng Wang<sup>a</sup>, Jinhai Cui<sup>a</sup>, Xingwang Zhu<sup>b\*</sup> and Kostya (Ken) Ostrikov<sup>c</sup>*

<sup>a</sup>School of Chemistry and Chemical Engineering, Henan Key Laboratory of Biomolecular Recognition and Sensing, Henan D&A Engineering Center of Advanced Battery Materials, Shangqiu Normal University, Shangqiu 476000, China.

<sup>b</sup>School of the Environment and Safety Engineering, Jiangsu University, Zhenjiang, Jiangsu, 212013, China.

<sup>c</sup>School of Chemistry and Physics and Centre for Materials Science, Queensland University of Technology, Brisbane, QLD 4000, Australia.

\*Corresponding authors E-mail: [wxchenedu@163.com](mailto:wxchenedu@163.com), [zxwiii@sina.com](mailto:zxwiii@sina.com)

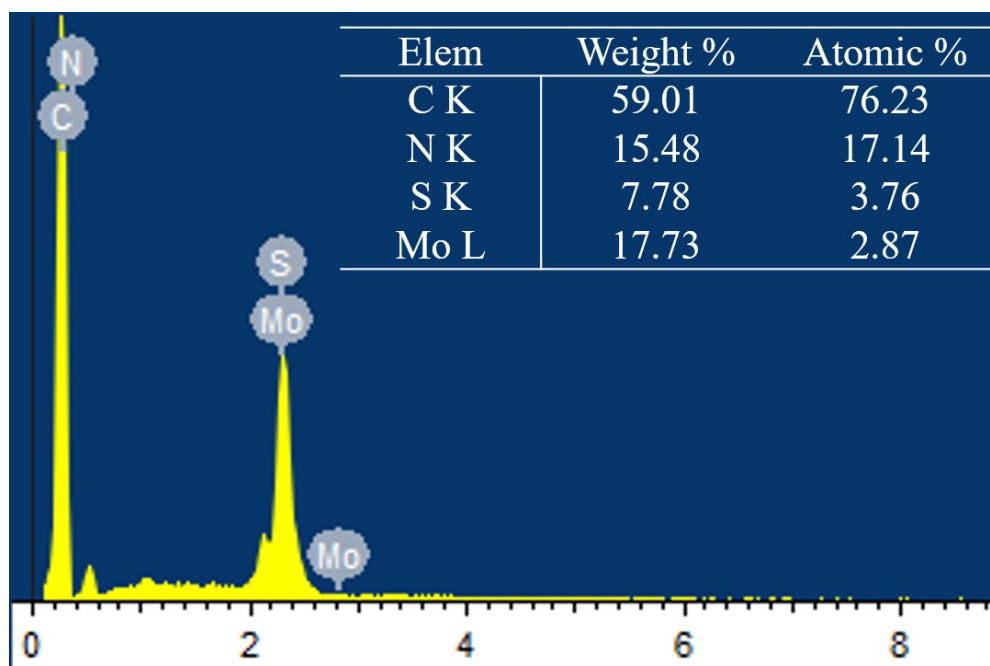


**Fig. S1.** The EDX spectral analysis of the C-N-MoS<sub>2</sub>/CC-700 material.

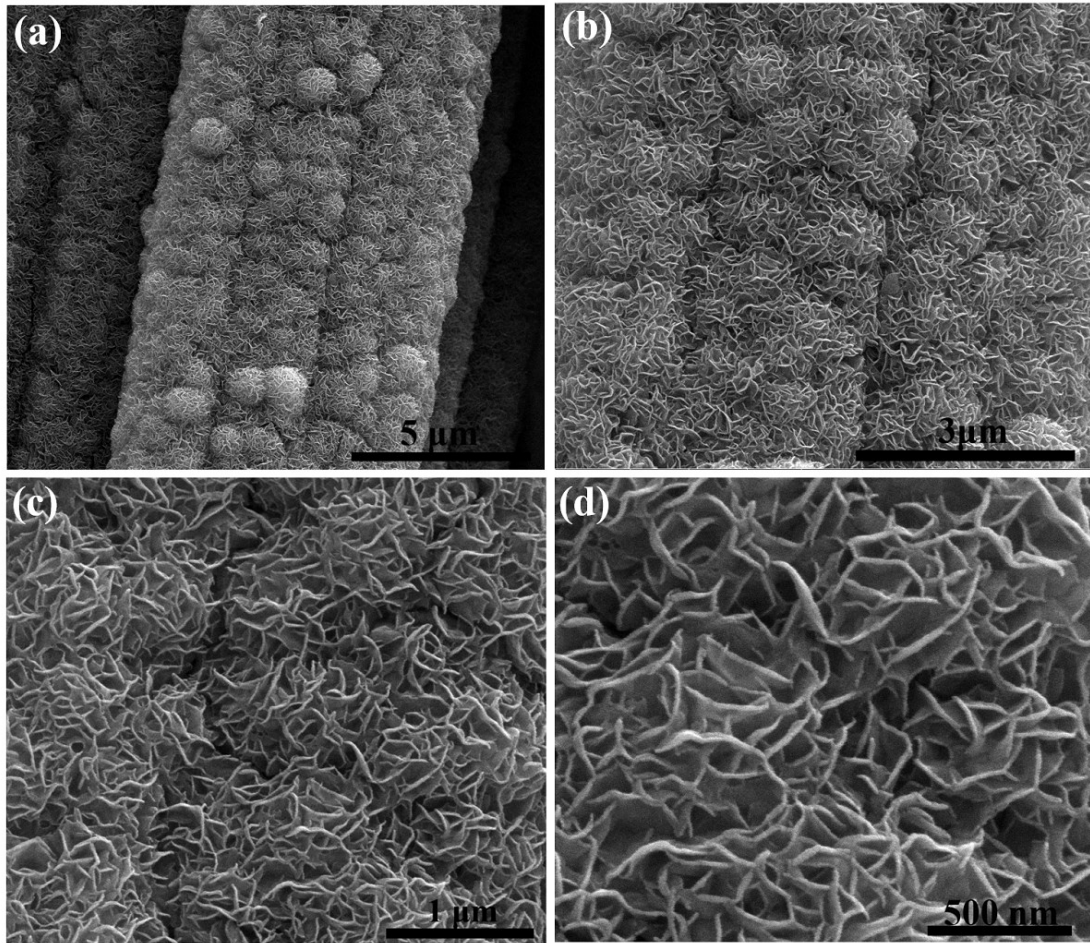


**Fig. S2.** The SEM image of the pure MoS<sub>2</sub>/CC.

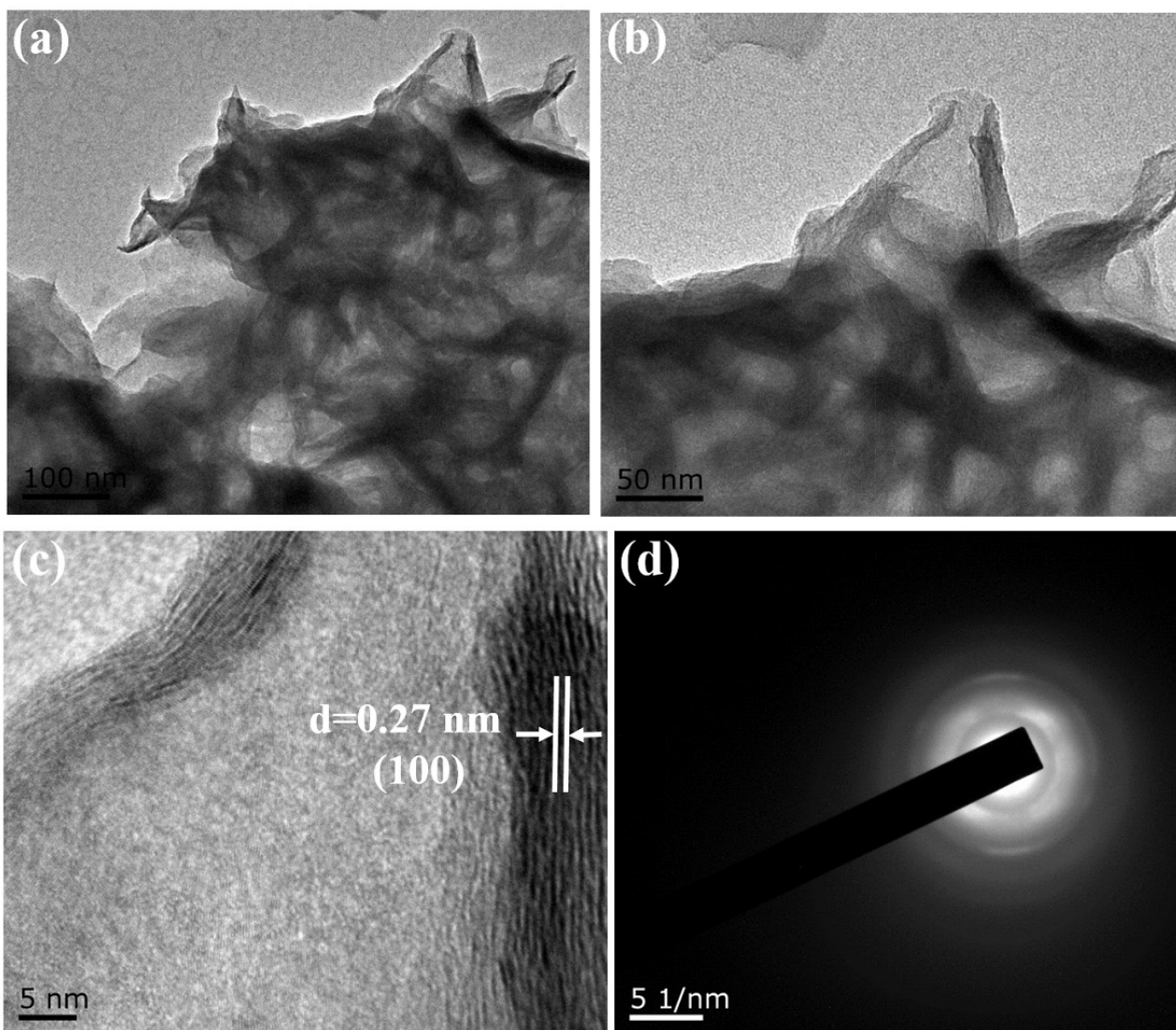


**Fig. S3.** (a) and (b) TEM image, (c) HRTEM image and (d) electron diffraction of the pure MoS<sub>2</sub>/CC.

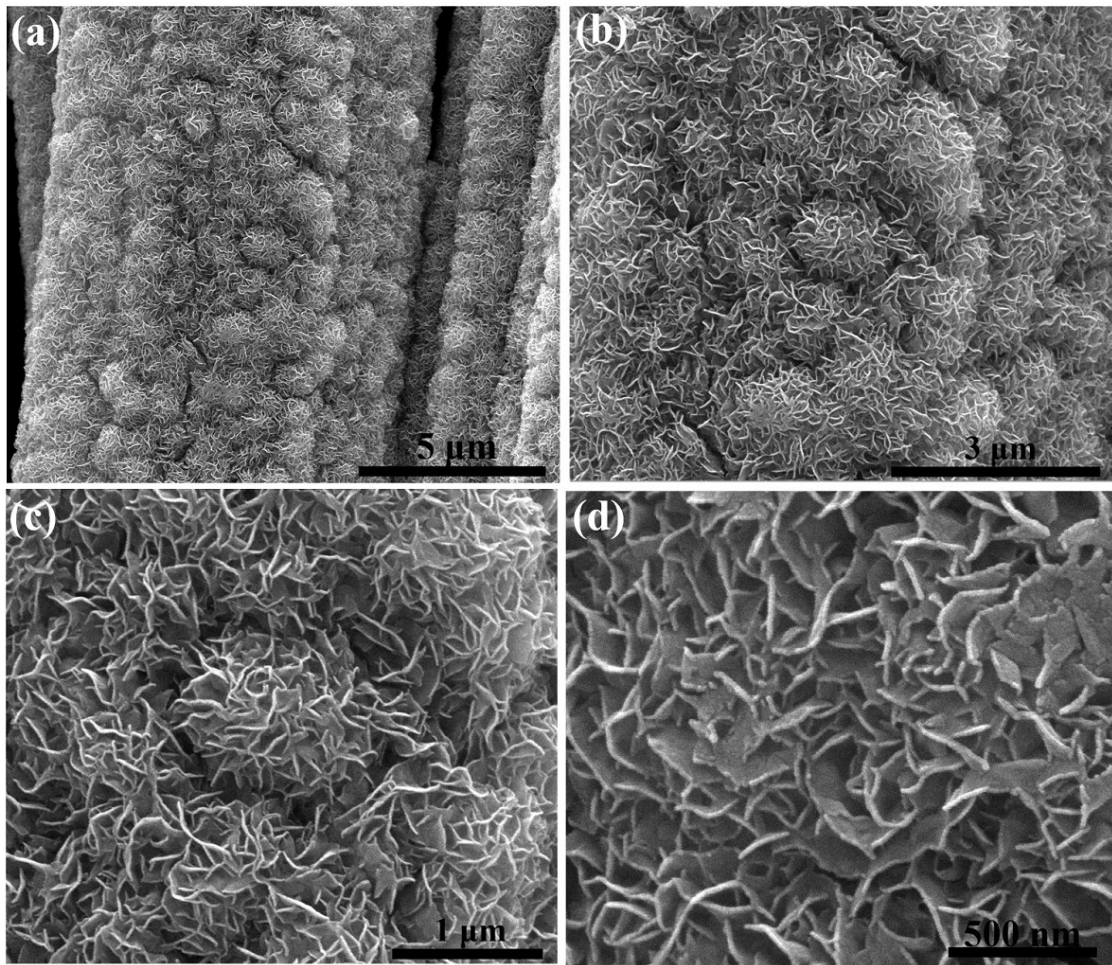


**Fig. S4.** The SEM image of the C-N-MoS<sub>2</sub>/CC-550.

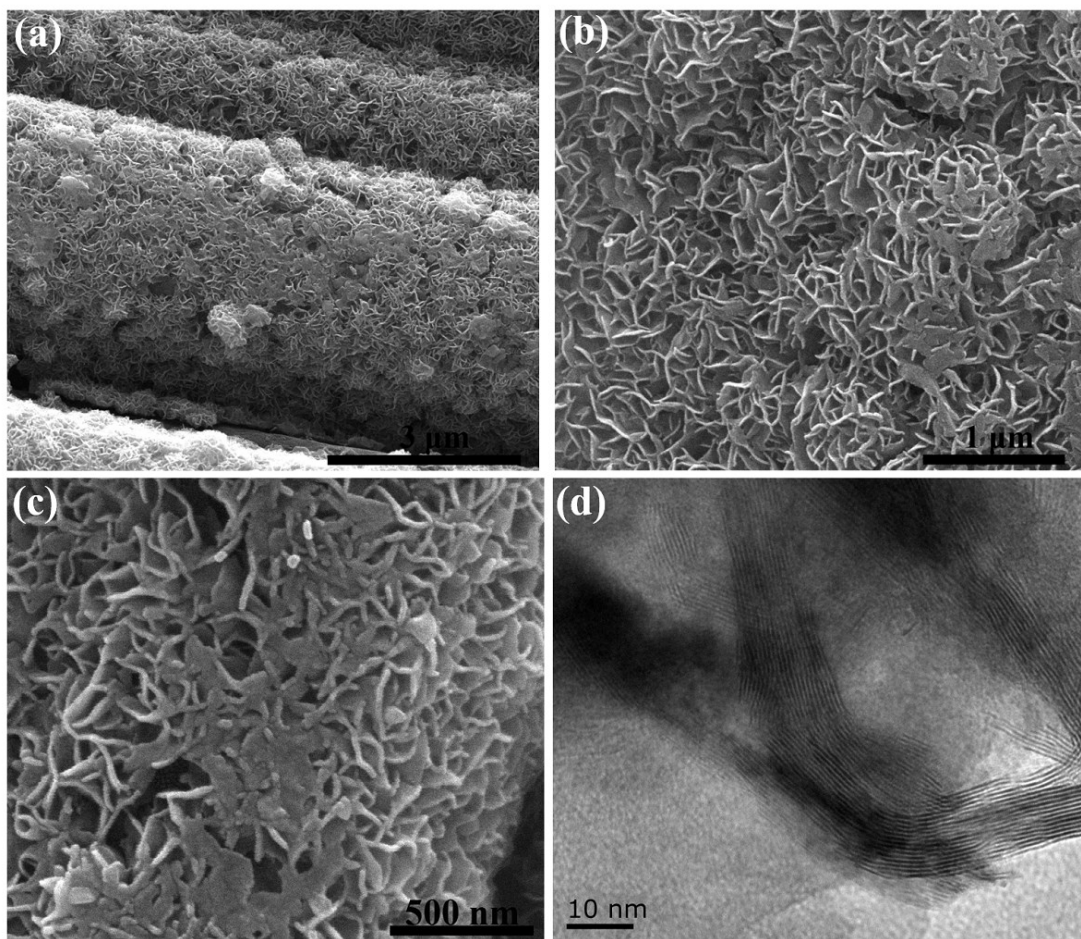


**Fig. S5.** The SEM image of the C-N-MoS<sub>2</sub>/CC-600.

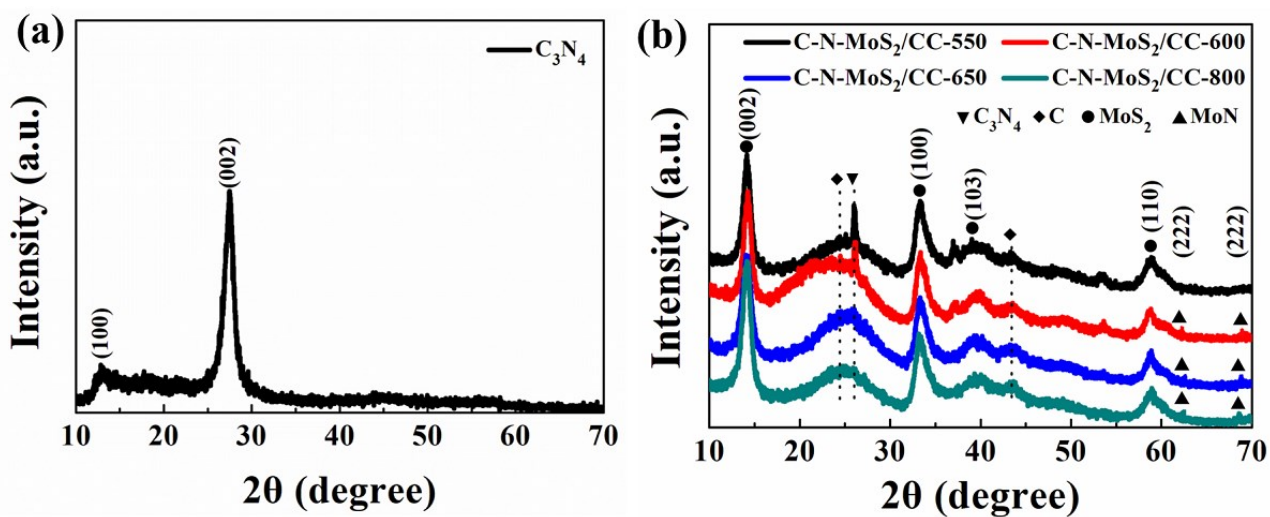


**Fig. S6.** The XRD patterns of the as-prepared catalyst: (a)  $C_3N_4$ , (b)  $C-N-MoS_2/CC-550$ ,  $C-N-MoS_2/CC-600$ ,  $C-N-MoS_2/CC-650$  and  $C-N-MoS_2/CC-800$ .

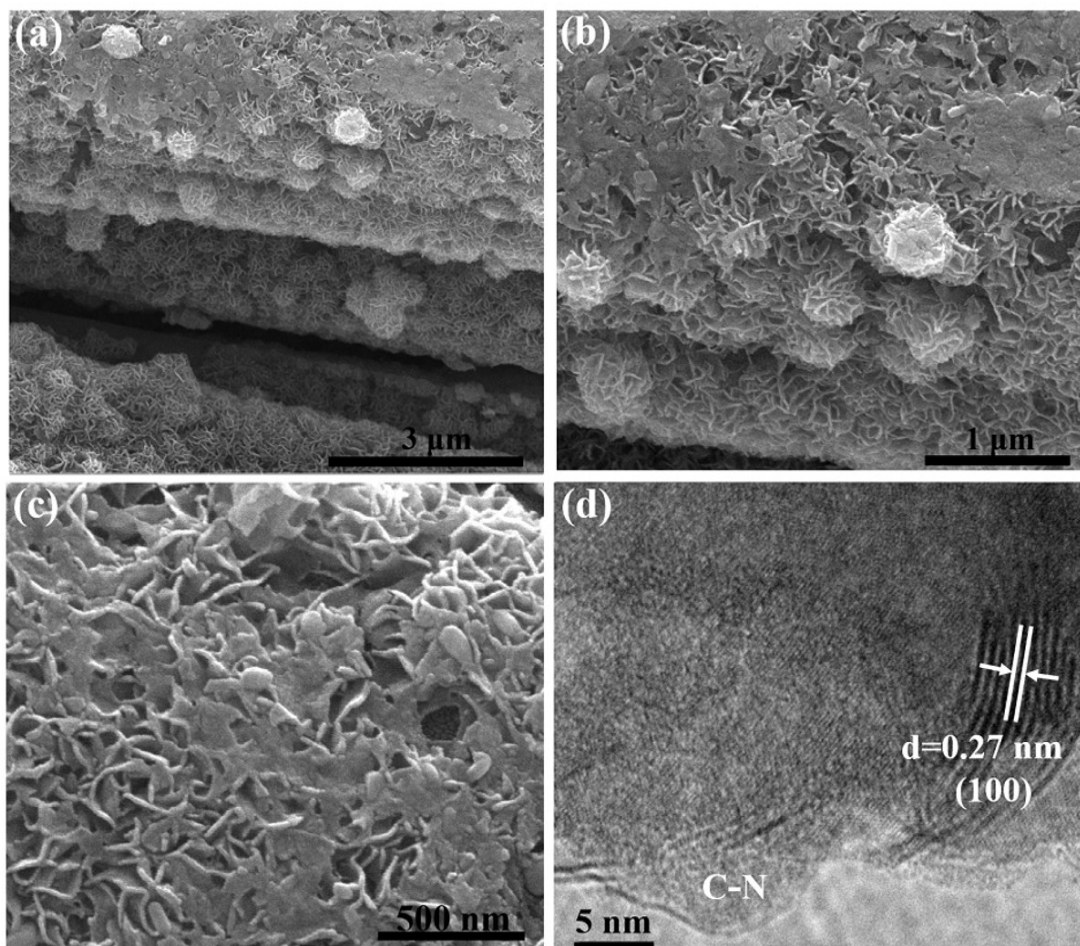


**Fig. S7.** (a), (b) and (c) The SEM image of the C-N-MoS<sub>2</sub>/CC-650, (d) The TEM image of the C-N-MoS<sub>2</sub>/CC-650.



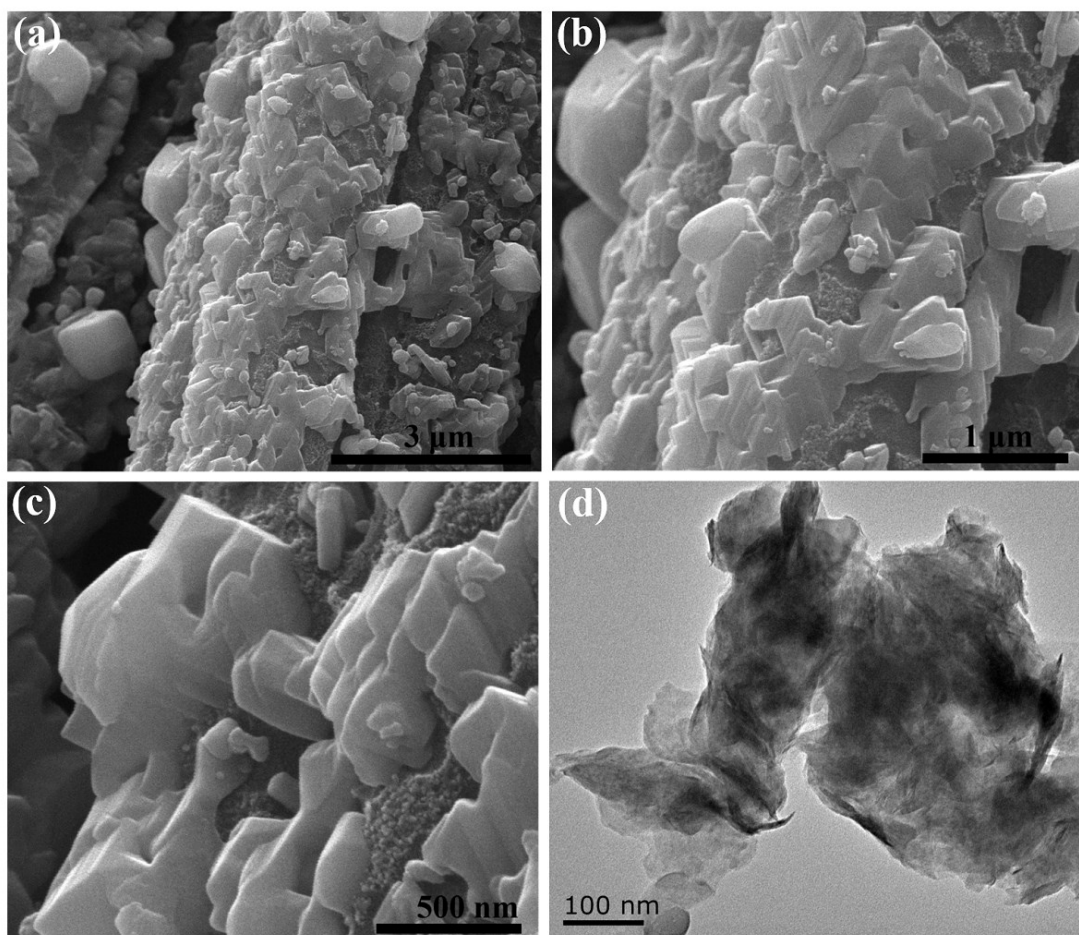


**Fig. S8.** (a), (b) and (c) The SEM image of the C-N-MoS<sub>2</sub>/CC-800, (d) The TEM image of the C-N-MoS<sub>2</sub>/CC-800.

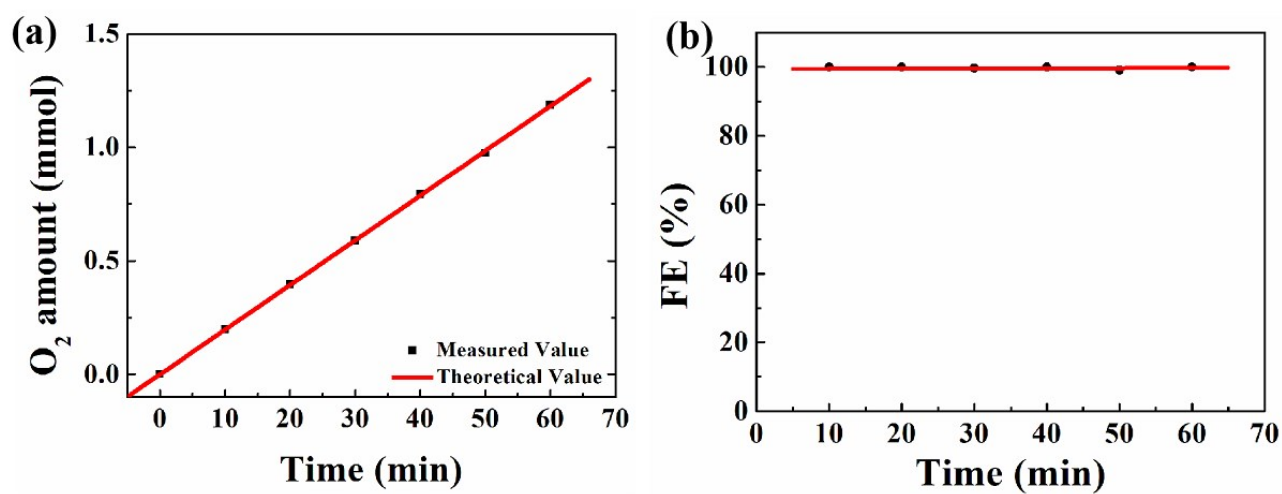


**Fig. S9.** (a) The O<sub>2</sub> amount of C-N-MoS<sub>2</sub>/CC-700 generated at a current density of 10 mA cm<sup>-2</sup> and (b) corresponding Faraday efficiency.

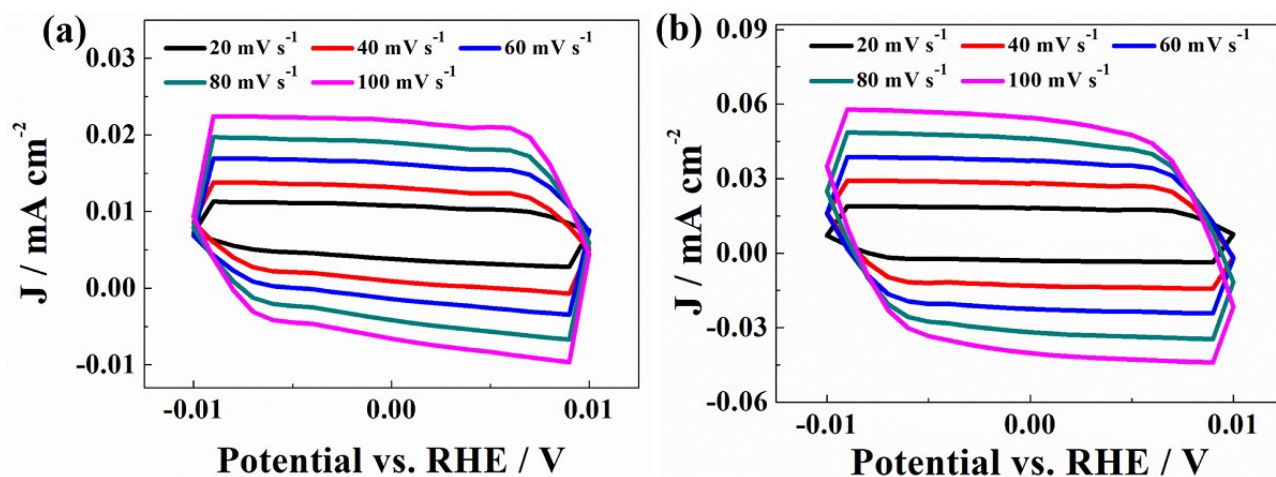


**Fig. S10.** CV curves at various scan rates in the potential range -0.01~0.01 V vs. RHE for (a) MoS<sub>2</sub>/CC, (b) C-N-MoS<sub>2</sub>/CC-700, respectively.

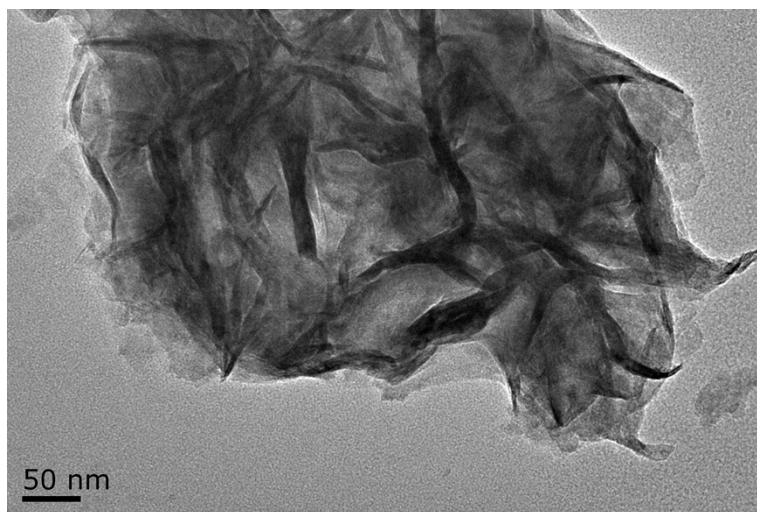


**Fig. S11.** The TEM image of the C-N-MoS<sub>2</sub>/CC-700 after OER.

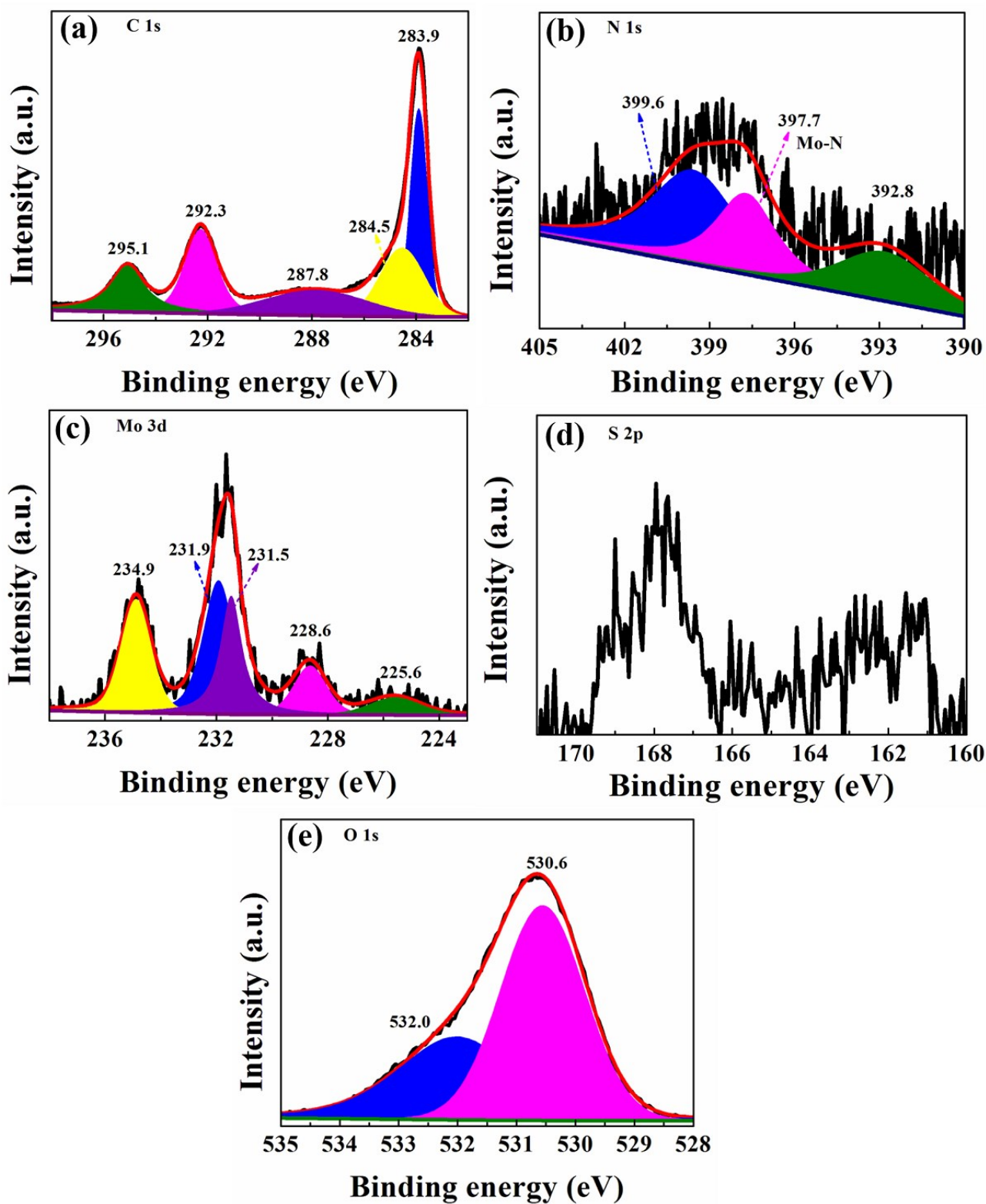
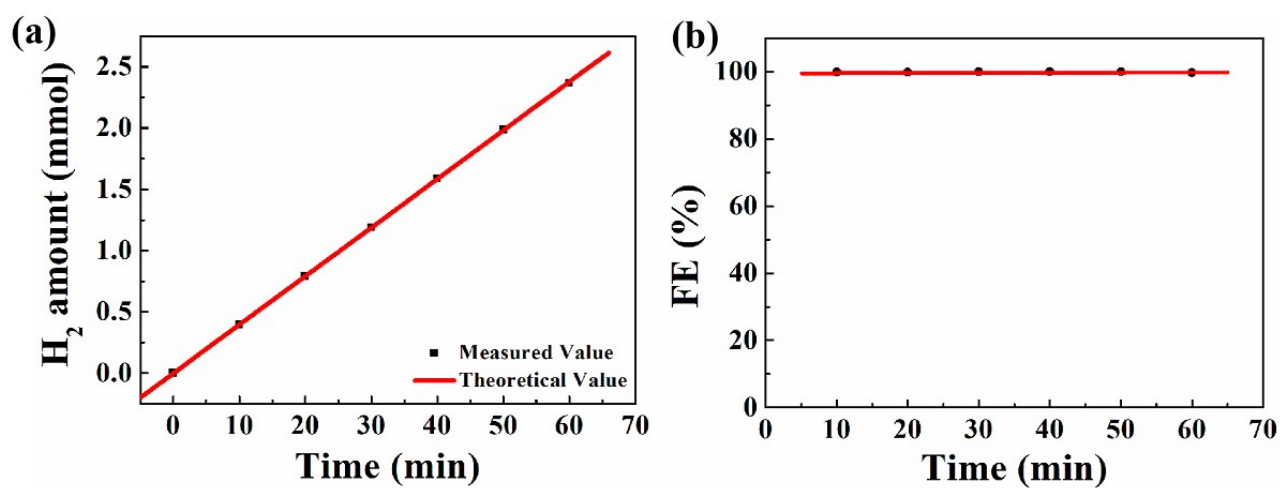
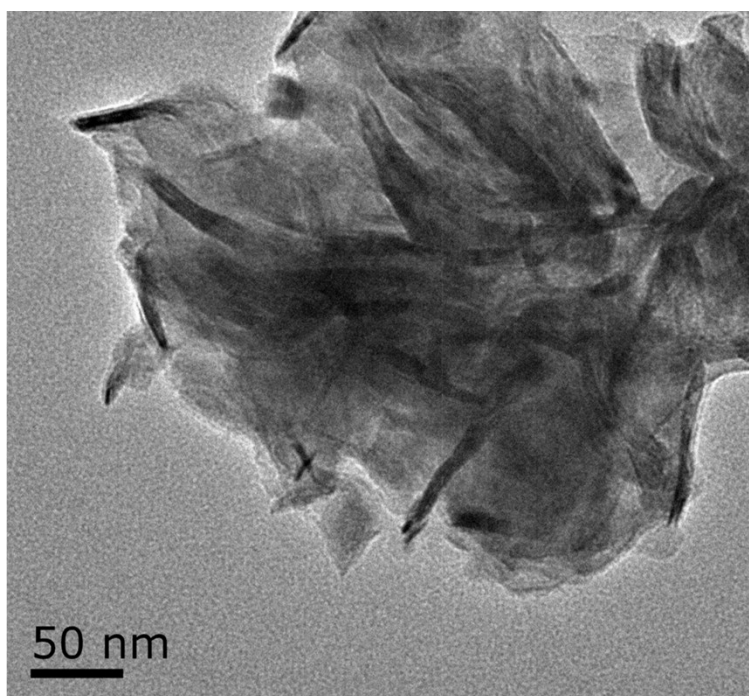


Fig. S12. The XPS spectra of the C-N-MoS<sub>2</sub>/CC-700 after OER.



**Fig. S13.** (a) The H<sub>2</sub> amount of C-N-MoS<sub>2</sub>/CC-700 generated at a current density of 10 mA cm<sup>-2</sup> and (b) corresponding Faraday efficiency.



**Fig. S14.** The TEM image of the C-N-MoS<sub>2</sub>/CC-700 after HER.

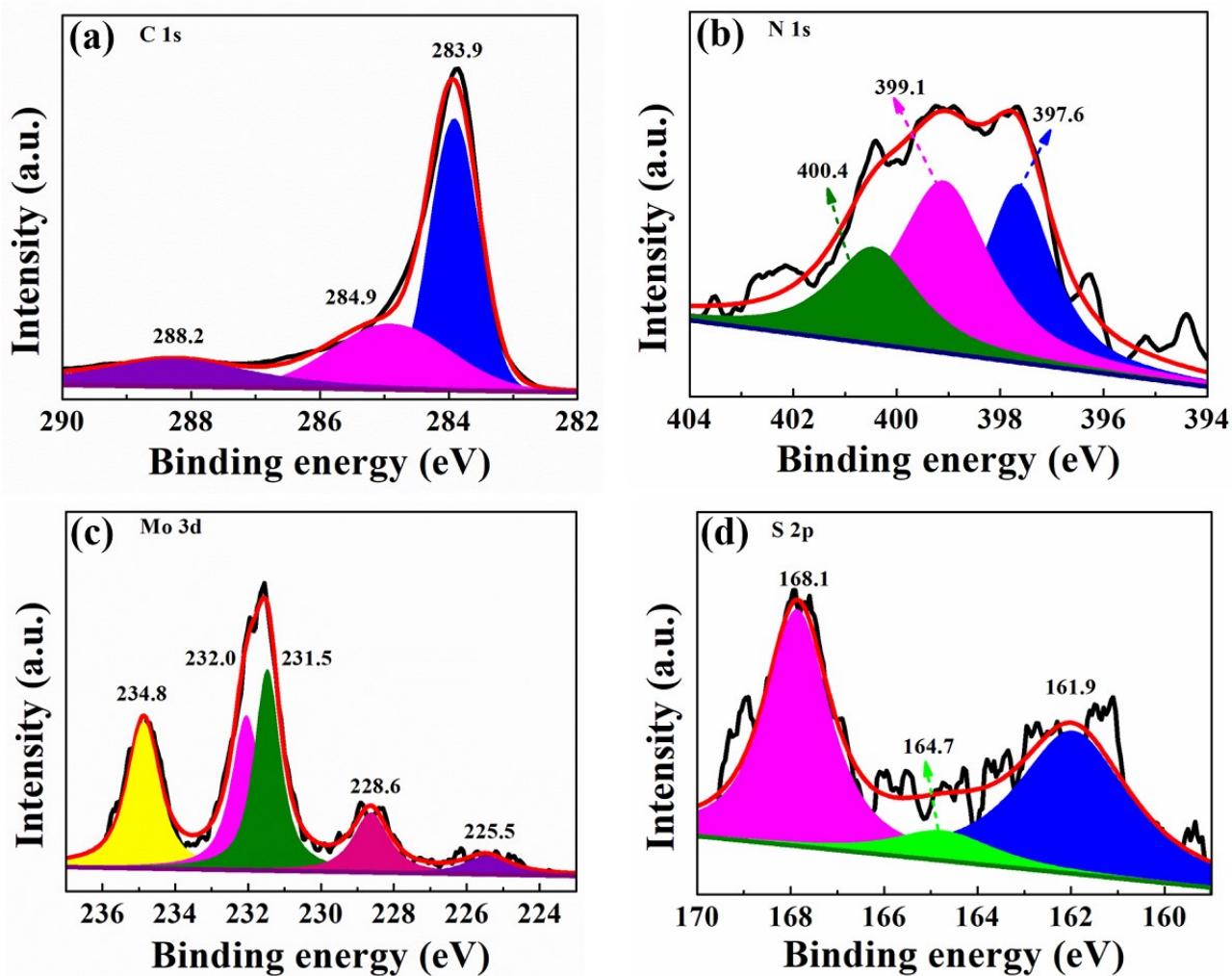
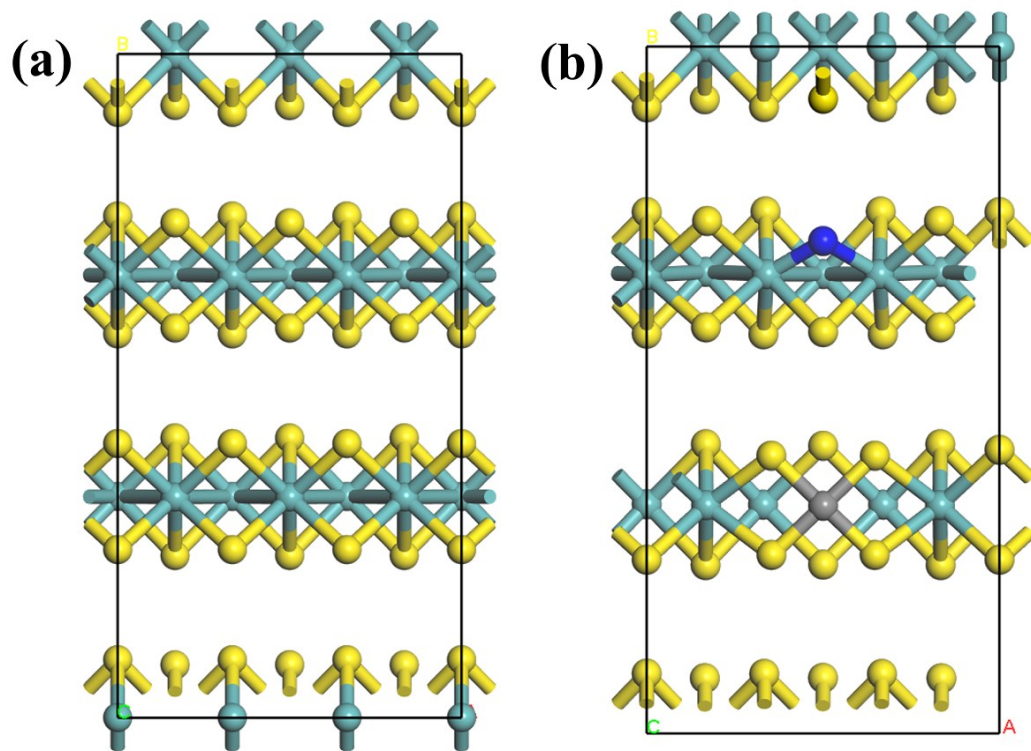
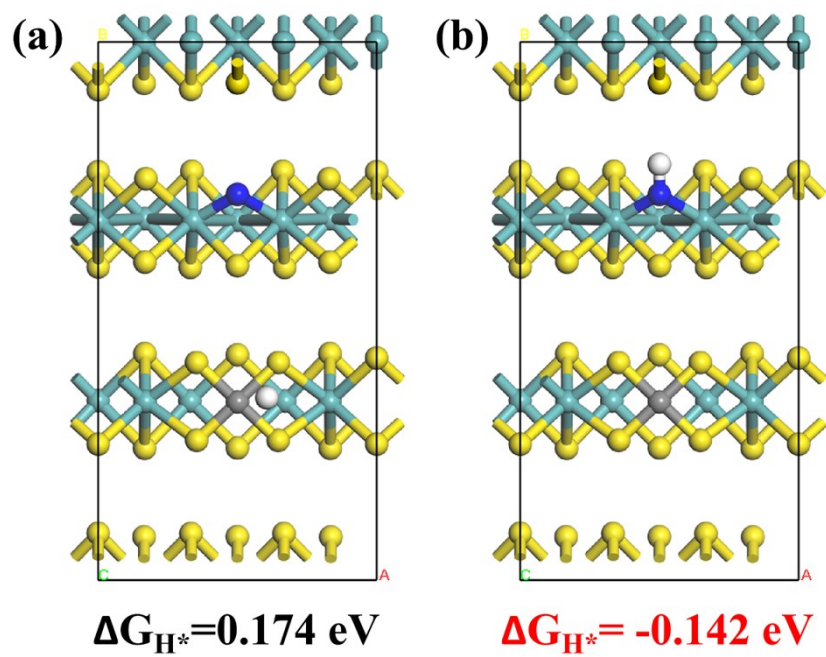


Fig. S15. The XPS spectra of the C-N-MoS<sub>2</sub>/CC-700 after HER.





**Fig. S16.** The optimized atomic structure model for (a) MoS<sub>2</sub> and (b) C-N-MoS<sub>2</sub>-700.



**Fig. S17.** The influence of different adsorption active sites.

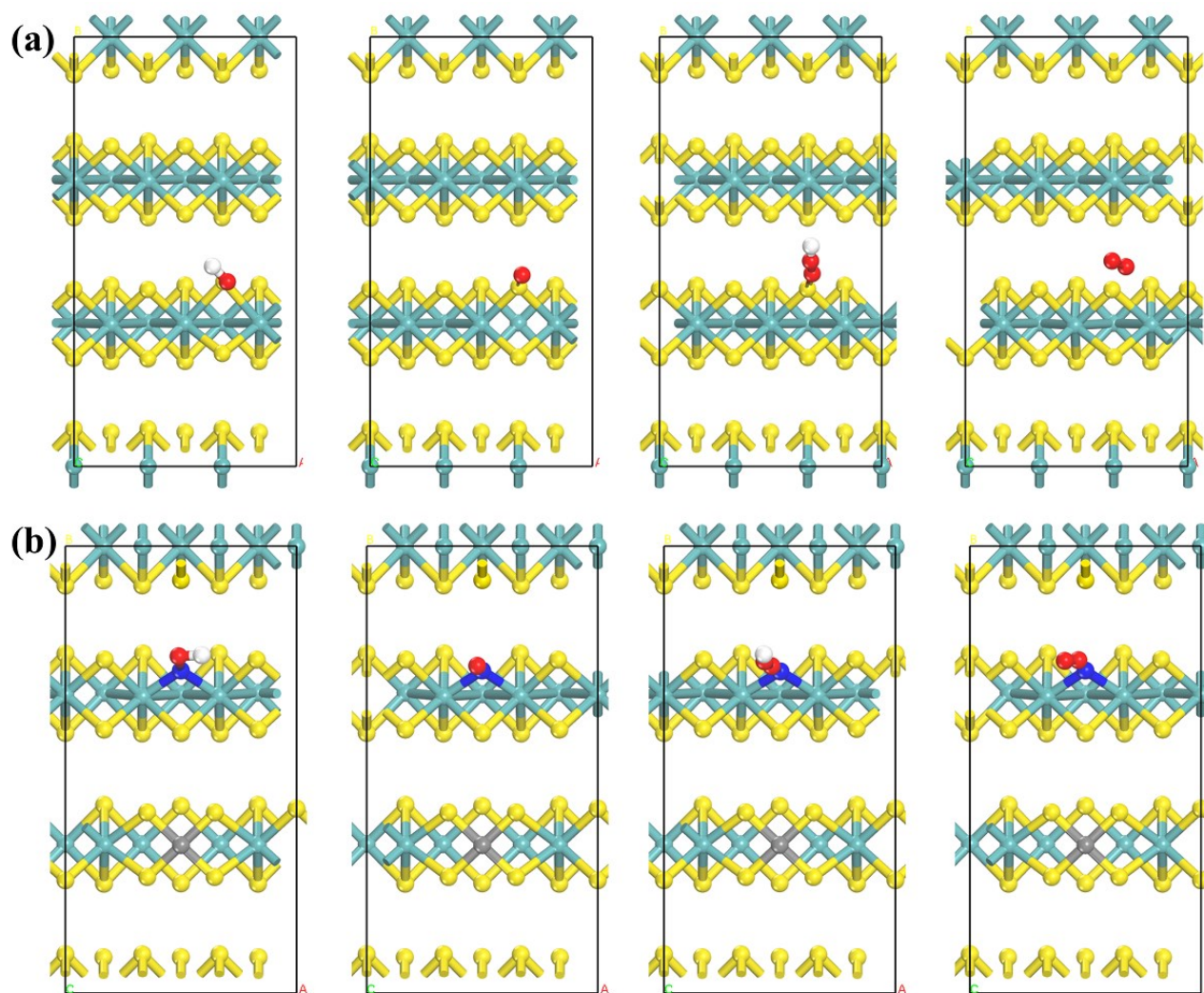


**Fig. S18.** The intermediates configuration of OER for (a) pure MoS<sub>2</sub> and (b) C-N-MoS<sub>2</sub>-700.

Table S1 The atomic ratio of the prepared catalyst analyzed by XPS.

Sample	Atomic concentration (%)				Atomic ratio
	C	N	Mo	S	C/N
<b>C-N-MoS<sub>2</sub>/CC-550</b>	53.77	38.67	3.14	4.42	1.4
<b>C-N-MoS<sub>2</sub>/CC-600</b>	62.71	30.29	3.02	3.98	2.1
<b>C-N-MoS<sub>2</sub>/CC-650</b>	67.32	25.80	2.99	3.89	2.6
<b>C-N-MoS<sub>2</sub>/CC-700</b>	74.39	18.98	2.87	3.76	3.9
<b>C-N-MoS<sub>2</sub>/CC-800</b>	77.14	16.17	2.90	3.79	4.8

**Table S2** The comparison of OER performance with state-of-the-art electrocatalysts.

Materials	Supports	Electrolytes	$\eta_{J=10 \text{ mA cm}^{-2}}$ (mV)	References
CN-MoS <sub>2</sub> /CC-700	CC	1 M KOH	230	This work
MoS <sub>2</sub> /NiS	GC	1 M KOH	350	1
CoNC@MoS <sub>2</sub> /CNF	GC	1 M KOH	325	2
Co(OH) <sub>2</sub> @aMoS <sub>2+x</sub>	-	1 M KOH	380	3
Co <sub>9</sub> S <sub>8</sub> @MoS <sub>2</sub> /CNFs	-	1 M KOH	430	4
MoS <sub>2</sub> -Ni <sub>3</sub> S <sub>2</sub> HNRs	NF	1 M KOH	249	5

**Table S3** TOF of the as-prepared catalysts at overpotential of 200, 250 and 300 mV corresponding to OER.

<b>TOF s<sup>-1</sup>(mV)</b> <b>Samples</b>	<b><math>\eta=200</math></b>	<b>250</b>	<b>300</b>
<b>MoS<sub>2</sub>/CC</b>	0.00843	0.0120	0.0150
<b>C-N-MoS<sub>2</sub>/CC-550</b>	0.0201	0.0294	0.0375
<b>C-N-MoS<sub>2</sub>/CC-600</b>	0.0326	0.0494	0.0821
<b>C-N-MoS<sub>2</sub>/CC-650</b>	0.0471	0.0657	0.1050
<b>C-N-MoS<sub>2</sub>/CC-700</b>	0.0827	0.1260	0.1530
<b>C-N-MoS<sub>2</sub>/CC-800</b>	0.0122	0.0150	0.0179

**Table S4** The comparison of HER performance with state-of-the-art electrocatalysts.

Materials	Supports	Electrolytes	$\eta_{J=10 \text{ mA cm}^{-2}}$ (mV)	References
C-N-MoS <sub>2</sub> /CC-700	CC	1 M KOH	90	This work
MoS <sub>2+x</sub> nanoparticles	-	1M KOH	310	1
CoNC@MoS <sub>2</sub> /CNF	CC	1M KOH	143	2
MoS <sub>2</sub> /NiCoS	GC	1 M KOH	189	6
MoS <sub>2</sub> /NiS	GC	1 M KOH	244	7
CoS <sub>x</sub> @MoS <sub>2</sub>	Ni foil	1 M KOH	146	8
MoS <sub>2</sub> @CoO	CC	1 M KOH	325	9
NiS <sub>2</sub> /MoS <sub>2</sub>	GC	1 M KOH	204	10
OGNs@MoS <sub>2</sub> -40	-	1M KOH	125	11

**Table S5** TOF of the as-prepared catalysts at overpotential of 200, 250 and 300 mV corresponding to HER.

<b>TOF s<sup>-1</sup>(mV)</b> <b>Samples</b>	<b><math>\eta=200</math></b>	<b>250</b>	<b>300</b>
<b>MoS<sub>2</sub>/CC</b>	0.00985	0.0190	0.0250
<b>C-N-MoS<sub>2</sub>/CC-550</b>	0.0269	0.0334	0.0415
<b>C-N-MoS<sub>2</sub>/CC-600</b>	0.0386	0.0586	0.0861
<b>C-N-MoS<sub>2</sub>/CC-650</b>	0.0651	0.0889	0.1190
<b>C-N-MoS<sub>2</sub>/CC-700</b>	0.1130	0.1470	0.1860
<b>C-N-MoS<sub>2</sub>/CC-800</b>	0.0181	0.0223	0.0272



## References

- 1 C. G. Morales-Guio, L. Liardet, M. T. Mayer, S. D. Tilley, M. Grtzel, X. L. Hu, *Angew. Chem. Int. Ed.*, 2015, **54**, 664-667.
- 2 D. X. Ji, S. J. Peng, L. Fan, L. L. Li, X. H. Qin and S. Ramakrishna, *J. Mater. Chem. A*, 2017, **5**, 23898-23908.
- 3 T. Yoon, K. S. Kim, *Adv. Funct. Mater.*, 2016, **26**, 7386-7393.
- 4 H. Zhu, J. F. Zhang, Y. zhang, M. L. Du, Q. F. Wang, *Adv. Mater.*, 2015, **27**, 4752-4759.
- 5 Y. Q. Yang, K. Zhang, H. L. Lin, X. Li, H. C. Chan, L. C. Yang, Q. S. Gao, *ACS Catal.*, 2017, **7**, 2357-2366.
- 6 C. L. Qin, A. X. Fan, X. Zhang, S. Q. Wang, X. L. Yuan and X. P. Dai. *J. Mater. Chem. A*, 2019, **7**, 27594-27602.
- 7 Q. Qin, L. Chen, T. Wei and X. Liu, *Small*, 2019, **15**, 1803639.
- 8 S. Shit, S. Chhetri, S. Bolar, N. C. Murmu, W. Jang, H. Koo and T. Kuila, *ChemElectroChem*, 2019, **6**, 430-438.
- 9 P. Cheng, C. Yuan, Q. Zhou, X. Hu, J. Li, X. Lin, X. Wang, M. Jin, L. Shui and X. Gao, *J. Phys. Chem. C*, 2019, **123**, 5833-5839.
- 10 P. Kuang, T. Tong, K. Fan and J. Yu, *ACS Catal.*, 2017, **7**, 6179-6187.
- 11 V. T. Nguyen, P. A. A. Le, Y. C. Hsu, K. H. Wei. *ACS Appl. Mater. Interfaces*, 2020, **12**, 11533-11542.